

Instability study of an annular liquid sheet of polymer produced by atomization.

Edgar P. Herrero; E.M.M. Del Valle^a and M.A. Galán.

Dep. Chem. Eng. Univ. of Salamanca, P/Los Caídos, 37008, Salamanca, Spain; ^aemvalle@usal.es

1. Summary

A temporal stability analysis was carried out to model the atomization of a swirling viscous annular liquid sheet emanating from an air-blast atomizer subject to inner and outer inviscid swirling air streams. The dimensionless dispersion equation that governs the instability of a viscous annular liquid sheet under swirling air streams was obtained. Numerical solutions to the dispersion equation under a wide range of flow conditions were obtained to investigate the effect of the liquid and gas flow on the maximum growth rate and its corresponding unstable wave number. The theoretical behaviour predicted by the dispersion diagrams was compared with the experimental results obtained by the same authors in previous works from the atomization of alginate solution using an air-blast atomizer. It was found that the instability model proposed justify the experimental effects found for the atomization of the fluid and under the work range for alginate flow rate and viscosity and air flow rate.

Keywords: atomization; air-blast atomizer; instability; growth rate

2. Introduction

The process of transforming bulk liquid into a large number of droplets and dispersing them in the form of a spray in a gaseous environment is called as atomization. Liquid atomization is of importance in numerous applications such as fuel injection in engines, crop spraying, food drying, manufacturing of pharmaceutical products, and lately microencapsulation applications [1].

During the last decade atomization techniques as air-blast or twin-fluid atomization has been widely used [2-4]. In air-blast atomization, low-speed liquid jets are accelerated by the surrounding high-speed gas flow, usually in the spray flow direction. The liquid is subjected to both tensile and shearing stresses. The magnitude of the extension has been shown to be significant for applications involving polymer solutions. Twin-fluid atomizers have a number of advantages over pressure atomizers including lower requirements for the liquid injection pressure and finer sprays.

Unfortunately, the process of air-blast atomization is very complex and its physical mechanisms are not fully understood [1].

Theoretical and experimental studies on the mechanism of atomization have been carried out by Rayleigh, Tyler, Weber, Haenlein, Ohnesorge and Castleman [1]. Detailed reviews of earlier work have been published by Giffen and Muraszew [5], and more recently by Chigier [6], and Lefebvre [1] from these studies it can be concluded that the wave mechanism has been found the widest acceptance among the mechanisms of atomization. According to this theory the disintegration of liquid sheets or liquid jets is caused by the growth of unstable waves at the liquid-gas interface due to the aerodynamic interactions between the liquid and the gas. This type of instability is referred to as Kelvin-Helmholtz instability [7] and is characterized by unstable waves that appear in the fluid interface between two superimposed fluids of differing densities and velocities.

The waves are generated by factors such as pressure fluctuations or turbulence in the gas stream or liquid stream [8-9]. Due to aerodynamic interactions, the perturbations grow in magnitude and reach a maximum value. When the dynamic pressure ($\rho_a U_a^2 / 2$) of the air stream in air-blast atomization is large enough, the amplitude of the surface waves will grow if their wavelength (λ) exceeds a minimum value [8-11]. There exists a dominant or most unstable wave number corresponding to the maximum growth rate and when the amplitude of the disturbance reaches a critical value, the wave detaches from the sheet to form ligaments, which rapidly collapse, forming drops.

E. P. Herrero et. al. [12], based on atomization processes, have developed a new technology of production of microcapsules based on a non-Newtonian fluid alginate solutions, which produced microcapsules ranged between 1-50 microns, with control size and a particle size distribution with a relative span factor, $(D_{0.9}-D_{0.1})/D_{0.5}$, less than 1.4. They have studied the effect of the alginate solution viscosity and flow rate and air flow rate. They have also developed a mathematical semi-empirical model, based on the wave mechanism, to predict the size of the microcapsules produced by atomization [13].

Therefore, the main aim of this work is to develop a temporal stability analysis to model the atomization of a swirling viscous annular liquid sheet emanating from an air-blast atomizer subject to inner and outer inviscid swirling air streams. The dimensionless dispersion equation that governs the instability of a viscous annular liquid sheet under swirling air streams will be derived. Usually this equation is derived and solved for an inviscid liquid sheet, because this analysis should be used to improve the fuel atomization in aircraft engines. The elimination of the liquid viscosity in the main equations does not affect very much the solution in this case. In microencapsulation application, where polymers are used the viscosity can not be eliminated because is a very important parameter especially when the polymer has a non-Newtonian behaviour, however in this work low polymer concentration have been used, therefore it would be possible to consider the fluid as a Newtonian liquid [14]. For that reason, numerical solutions to the dispersion equation under a wide range of liquid viscosity values, and flow conditions will be carried out to investigate the effects of the liquid and gas on the maximum growth rate and its corresponding

Instability study of an annular liquid sheet of polymer produced by atomization.

unstable wave number. So, the theoretical behaviour predicted by the dispersion diagrams will be compared with the experimental results obtained previously from the atomization of alginate solution, using an air-blast atomizer.

3. Linear stability analysis.

3.1. Model assumptions.

The stability model considers a swirling viscous annular liquid sheet subject swirling airstreams as shown in Figure 1. Gas phases are assumed to be inviscid and incompressible. The basic flow velocities for liquid, inner gas and outer gas are assumed to be $(U_l, 0, A_l / r)$, $(U_i, 0, \Omega r)$, $(U_o, 0, A_o / r)$ respectively. Inner gas swirl profile is assumed to be solid body rotation and outer gas swirl profile is of free vortex type. The assumed velocity profiles are similar to the profiles in an air blast atomizer [15].

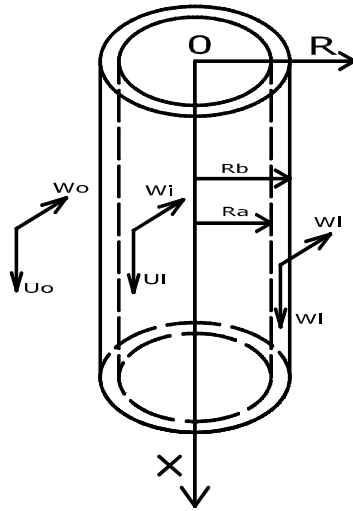


Figure 1: annular swirling viscous liquid sheet subject to swirling airstreams

Sheet instability occurs due to the growth of unstable waves at the liquid gas interface. The growth rates of these unstable waves are governed by fluid properties, nozzle geometry and competition of forces acting on the interface including viscous, pressure, inertial, surface tension, and centrifugal force. There exists a dominant or most unstable wave number corresponding to the maximum growth rate. A temporal linear instability analysis is conducted to determine the maximum growth rate and the most unstable wave number.

3.2. Linearized disturbance equations.

The governing equations for viscous annular fluid flows are the continuity and Navier-Stokes equations that in cylindrical coordinate system are:

Continuity:

$$\frac{V}{r} + \frac{\partial V}{\partial r} + \frac{1}{r} \frac{\partial W}{\partial \theta} + \frac{\partial U}{\partial x} = 0 \quad (1)$$

Momentum:

$$\frac{\partial U}{\partial t} + V \frac{\partial U}{\partial r} + \frac{W}{r} \frac{\partial U}{\partial \theta} + U \frac{\partial U}{\partial x} = \frac{-1}{\rho} \frac{\partial p}{\partial x} + \nu \left(\frac{\partial^2 U}{\partial r^2} + \frac{1}{r} \frac{\partial U}{\partial r} + \frac{1}{r^2} \frac{\partial^2 U}{\partial \theta^2} + \frac{\partial^2 U}{\partial x^2} \right) \quad (2)$$

$$\frac{\partial V}{\partial t} + V \frac{\partial V}{\partial r} + \frac{W}{r} \frac{\partial V}{\partial \theta} + U \frac{\partial V}{\partial x} - \frac{W^2}{r} = \frac{-1}{\rho} \frac{\partial p}{\partial r} + \nu \left(\frac{\partial^2 V}{\partial r^2} + \frac{1}{r} \frac{\partial V}{\partial r} + \frac{1}{r^2} \frac{\partial^2 V}{\partial \theta^2} - \frac{V}{r^2} + \frac{2}{r^2} \frac{\partial W}{\partial \theta} + \frac{\partial^2 V}{\partial x^2} \right) \quad (3)$$

$$\frac{\partial W}{\partial t} + V \frac{\partial W}{\partial r} + \frac{W}{r} \frac{\partial W}{\partial \theta} + U \frac{\partial W}{\partial x} + \frac{VW}{r} = \frac{-1}{\rho} \frac{\partial p}{\partial \theta} + \nu \left(\frac{\partial^2 W}{\partial r^2} + \frac{1}{r} \frac{\partial W}{\partial r} + \frac{1}{r^2} \frac{\partial^2 W}{\partial \theta^2} - \frac{W}{r^2} + \frac{2}{r^2} \frac{\partial V}{\partial \theta} + \frac{\partial^2 W}{\partial x^2} \right) \quad (4)$$

In order to obtain the linearized disturbance equations, let:

$$U = \bar{U} + u, \quad V = v, \quad W = \bar{W} + w, \quad p = \bar{P} + p' \quad (5)$$

where, the overbar represents the mean flow quantities and u , v , w and p' indicates disturbances. The disturbances are assumed to be of the form:

$$(u, v, w, p') = (\hat{u}(r), \hat{v}(r), \hat{w}(r), \hat{p}(r)) e^{i(kx+n\theta-\omega t)} \quad (6)$$

where $\hat{}$ indicates the disturbance amplitude which is a function for r only. For the temporal analysis, the wave number k and n are real while frequency ω is complex. The maximum value of imaginary ω represents the maximum growth rate of the disturbance, and the corresponding value of k represents the most unstable wave number.

For such an annular jet, unstable waves develop on both the inner and outer surfaces, which may be in phase or out of phase. When the waves develop in phase, the shapes of the waves are antisymmetric with respect to the mid-plane of liquid sheet, and this kind of instability mode is called the para-sinusoidal mode (Figure 2a). When the waves develop out of phase, the waves are symmetric with respect to the mid-plane of the liquid sheet, and this mode is called the para-varicose mode (figure 2b) [16].

Instability study of an annular liquid sheet of polymer produced by atomization.

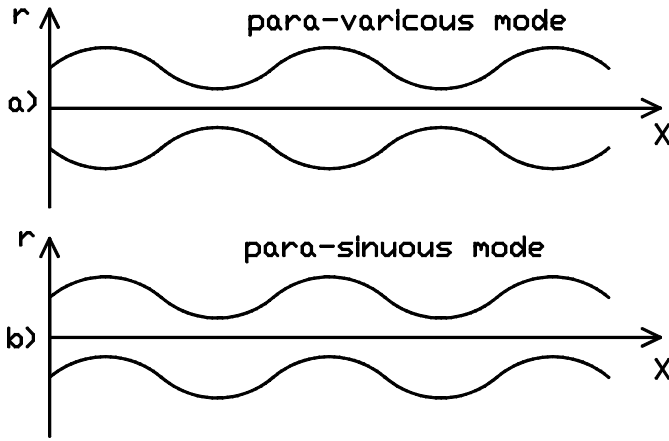


Figure 2: A schematic description of (a) the para-varicous mode and (b) the para-sinuuous mode.

The displacement disturbances at the inner and outer interfaces are given by the following equations:

$$\eta_i(x, \theta, t) = \eta_i e^{i(kx + n\theta - \omega t) + i\phi} \quad (7)$$

$$\eta_o(x, \theta, t) = \eta_o e^{i(kx + n\theta - \omega t)} \quad (8)$$

Here ϕ indicates the phase difference between the displacement at the inner and the outer interface.

Substituting Eq. 5 into Eq. 1, 2, 3 and 4, subtracting the mean flow equations and neglecting the second order terms, it is achieved the linearized equations for velocity and pressure disturbances.

In order to determine the effect of the various forces, properties of fluids and other geometric parameters, the linearized equations are non-dimensionlized by introducing the following dimensionless parameters:

$$\begin{aligned} We_l &= \frac{\rho_l U_l^2 D_b}{\sigma} & We_i &= \frac{\rho_i U_i^2 D_b}{\sigma} & We_o &= \frac{\rho_o U_o^2 D_b}{\sigma} & We_s &= \frac{\rho_l W_l^2 D_b}{\sigma} \\ We_{si} &= \frac{\rho_i W_i^2 D_b}{\sigma} & We_{so} &= \frac{\rho_o W_o^2 D_b}{\sigma} & Z &= \frac{\mu_l}{(\rho_l \sigma D_b)^{1/2}} & g_i &= \frac{\rho_i}{\rho_l} \\ g_o &= \frac{\rho_o}{\rho_l} & \bar{k} &= k R_b & \bar{\omega} &= \frac{\omega R_b}{U_l} & \frac{U_i}{U_l} &= \sqrt{\frac{We_i}{We_l} \frac{1}{g_i}} & \frac{U_o}{U_l} &= \sqrt{\frac{We_o}{We_l} \frac{1}{g_o}} \\ \frac{A_l}{U_l R_b} &= \sqrt{\frac{We_s}{We_l}} & \frac{A_o}{U_l R_b} &= \sqrt{\frac{We_{so}}{We_l} \frac{1}{g_o}} & \frac{\Omega R_b}{U_l} &= \sqrt{\frac{We_{si}}{We_l} \frac{1}{g_i}} \\ \bar{s} &= \left(\bar{k}^2 + Z(-i\bar{\omega} + i\bar{k}) \right)^{1/2} & h &= \frac{R_a}{R_b} \end{aligned}$$

As dimensionless parameters it has included the Weber number, which represents the ratio of aerodynamic force to surface tension, and the Ohnesorge number, which contains only the properties of the globules formed in primary atomization before they split up into smaller drops during secondary atomization. Ohnesorge number is sometimes called a stability group because it provides an indication of the resistance of a globule to further disintegration, but it is also called a viscosity group because it accounts for the effect of liquid viscosity on the globule. Ohnesorge number is used in momentum transfer in general and atomization calculations in particular.

Since it is considered three dimensional perturbations, the two surface waves may also be axisymmetric ($n = 0$) or non-axisymmetric ($n = 1$) with respect to the central axis of the jet. Several studies have examined the disintegration of non-swirling liquid sheets and liquid jets subject to axi-symmetric disturbances. Li and Tankin [17] conducted a temporal instability analysis of a thin viscous liquid sheet in an inviscid gas medium and found axi-symmetrical disturbances to control the instability process for small Weber numbers. Liao et al. [18] reported axi-symmetric mode to be the dominant mode in the absence of air swirl velocity. Chen et al. [19] carried out a linear stability analysis for an annular viscous jet subject to three dimensional disturbances and showed axisymmetric mode to be the most unstable mode in the system. As such we have restricted the present analysis to the axi-symmetric mode. Perturbation in the azimuthal direction is taken as zero i.e. $\hat{w} = 0$.

After applying these restrictions it is obtained the linearised disturbance equations for the liquid phase and the gas phase:

The disturbance equations for the liquid phase are:

$$\hat{u}(i\bar{k}) + \frac{d\hat{v}}{dr} + \frac{v}{r} = 0 \quad (9)$$

$$\hat{u}(-i\bar{\omega} + i\bar{k}) = -i\bar{k}\hat{p} + Z \left(\frac{d^2\hat{u}}{dr^2} + \frac{1}{r} \frac{d\hat{u}}{dr} - \frac{\hat{u}}{r^2} (k^2 r^2) \right) \quad (10)$$

$$\hat{v}(-i\bar{\omega} + i\bar{k}) = -\frac{d\hat{p}}{dr} + Z \left(\frac{d^2\hat{v}}{dr^2} + \frac{1}{r} \frac{d\hat{v}}{dr} - \frac{\hat{v}}{r^2} (k^2 r^2 + 1) \right) \quad (11)$$

The disturbance equations for the gas phase are,

Inner gas:

$$\hat{u}(i\bar{k}) + \frac{d\hat{v}}{dr} + \frac{v}{r} = 0 \quad (12)$$

Instability study of an annular liquid sheet of polymer produced by atomization.

$$\hat{u}\left(-i\bar{\omega}+i\bar{k}\sqrt{\frac{We_i}{We_l}\frac{1}{g_i}}\right)=-\frac{1}{g_i}i\bar{k}\hat{p} \quad (13)$$

$$\hat{v}\left(-i\bar{\omega}+i\bar{k}\sqrt{\frac{We_i}{We_l}\frac{1}{g_i}}\right)=-\frac{1}{g_i}\frac{d\hat{p}}{dr} \quad (14)$$

Outer gas:

$$\hat{u}(i\bar{k})+\frac{d\hat{v}}{dr}+\frac{v}{r}=0 \quad (15)$$

$$\hat{u}\left(-i\bar{\omega}+i\bar{k}\sqrt{\frac{We_o}{We_l}\frac{1}{g_o}}\right)=-\frac{1}{g_o}i\bar{k}\hat{p} \quad (16)$$

$$\hat{v}\left(-i\bar{\omega}+i\bar{k}\sqrt{\frac{We_o}{We_l}\frac{1}{g_i}}\right)=-\frac{1}{g_o}\frac{d\hat{p}}{dr} \quad (17)$$

3.3. Boundary conditions.

In the same way, under the above conditions, the following dimensionless boundary conditions are necessary to solve the linearized disturbance equations. The first boundary condition is the kinematic condition that a particle of fluid on the surface moves with the surface so as to remain on the surface or in other words, the velocity components normal to the interface is continuous across the interface,

Liquid:

$$v_l=\frac{\partial\eta_i}{\partial t}+\frac{\partial\eta_i}{\partial x} \quad \text{at } r=h \quad (18)$$

$$v_l=\frac{\partial\eta_o}{\partial t}+\frac{\partial\eta_o}{\partial x} \quad \text{at } r=1 \quad (19)$$

Inner gas:

$$v_i=\frac{\partial\eta_i}{\partial t}+\frac{\partial\eta_i}{\partial x}\sqrt{\frac{We_i}{We_l}\frac{1}{g_i}} \quad \text{at } r=h \quad (20)$$

Outer gas:

$$v_o=\frac{\partial\eta_o}{\partial t}+\frac{\partial\eta_o}{\partial x}\sqrt{\frac{We_o}{We_l}\frac{1}{g_o}} \quad \text{at } r=1 \quad (21)$$

Due to the inviscid assumption for the gas streams in the axial and azimuthal directions, viscous stress at the liquid-gas interface is zero. This is expressed as:

$$\frac{\partial u}{\partial r} + \frac{\partial v}{\partial x} = 0 \quad \text{at } r = h, 1 \quad (22)$$

The last boundary condition considers the balance between the surface stresses on both sides of the liquid-gas interface, including the pressure jump across the interface due to surface tension and viscous forces. This boundary condition is known as the dynamic boundary condition and is given by:

$$p_l' - p_i' = \frac{1}{h^2 We_l} \left(\eta_i + h^2 \frac{\partial^2 \eta_i}{\partial x^2} \right) + h \frac{We_{si}}{We_l} \eta_i - \frac{We_s}{We_l} \frac{\eta_i}{h^3} + 2Z \frac{\partial v}{\partial r} \quad \text{at } r = h \quad (23)$$

$$p_l' - p_o' = \frac{-1}{We_l} \left(\eta_o + \frac{\partial^2 \eta_o}{\partial x^2} \right) + \frac{We_{so}}{We_l} \eta_o - \frac{We_s}{We_l} \eta_o + 2Z \frac{\partial v}{\partial r} \quad \text{at } r = 1 \quad (24)$$

3.4. Non-dimensional dispersion equation.

By solving these equations and taking into account the boundary conditions, the final dimensionless dispersion equation was obtained

$$f(\bar{\omega}, \bar{k}, \bar{s}, g_i, g_o, Z, We_l, We_i, We_o, We_s, We_{si}, We_{so}, h) = 0 \quad (25)$$

The final dispersion equation was solved numerically using *Mathematica*TM. The Secant method is used where two starting complex guess values are required to determine the roots of the dimensionless dispersion equation. Results from the inviscid case are taken as starting guess values. By varying the value of k , it is solved for the root with the maximum imaginary part that represents the maximum growth rate of disturbance corresponding to the most unstable wave number.

4. Results and discussion.

In the process of determining the disintegration of the swirling viscous annular liquid sheet emanating from an air-blast prefilmer, the final non-linear dimensionless dispersion equation was derived based on the assumption that the inner and outer gas flows are inviscid moving axially outward with swirling velocity components. A complete parametric study has been conducted to insolate the effect of flow conditions and viscosity on the instability of the liquid sheet. The non-dimensional parameters utilized in the final dispersion equation are the axial Weber numbers, We_l , We_i , and We_o , swirling Weber numbers, We_s , We_{si} , and We_{so} , Ohnesorge number, Z , axial wave number k , gas to liquid air density ratio, g_i and g_o , and the annular liquid sheet inner and outer radii ratio, h .

The frequency with the maximum imaginary part represents the most unstable wave that is the perturbation that grows more rapidly than any other and for that reason it

Instability study of an annular liquid sheet of polymer produced by atomization.

dominates the liquid sheet breakup process. Therefore, the most unstable wave number is related to the mean drop size. The growth rate can be related to the breakup length of the liquid sheet. Higher growth rate indicates shorter breakup length. As such the most unstable wave number and the maximum growth rate are two important parameters that will determine the resulting spray characteristics. These parameters are obtained for a number of flow geometry conditions and are discussed below. The results are presented in three graphs (Figures 3, 4, and 5) $\omega = f(k)$ called dispersion diagrams. These figures show the expected bell shape, commonly encountered in linear theory analysis. In each situation, a finite range of unstable perturbations, i.e. showing a positive growth rate, was obtained.

a) Liquid flow rate variation:

The influence of the liquid flow rate variation in the growth rate is shown in Figure 3. These results were obtained for an atomization nozzle of 1.8 mm in previous works conducted by the authors [12]. The experimental conditions were the following: a constant value of pressurized flow air of 138.000 L/min ($We_i = We_o = We_{si} = We_{so} = 35128$) and the liquid flow rate was modified ranged from 0.003 l/min to 0.037 l/min ($We_l = We_s = 0.01$ to $We_l = We_s = 2$). The liquid viscosity was maintained constant at 64.5 mPa s ($Z = 0.2$). It can be seen in Figure 3 that when the liquid flow decrease, the growth rate increase, which indicates shorter breakup length and smaller drops.

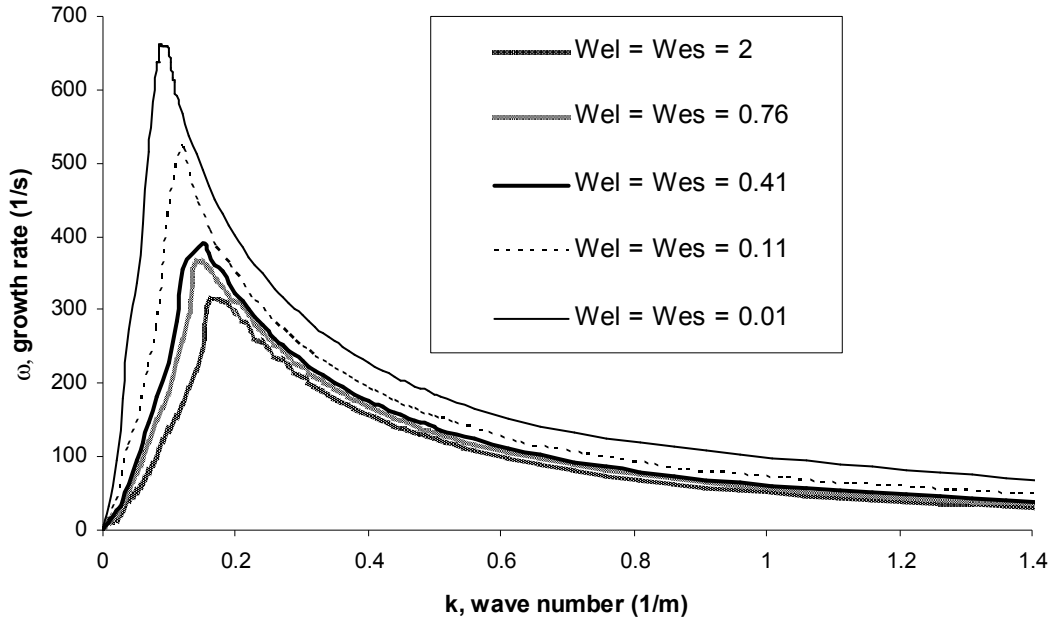


Figure 3: Dispersion diagram at

$We_i = We_o = We_{si} = We_{so} = 35128$; $Z = 0.2$

$We_l = We_s = 0.01 - 2$

These results are in a very good agreement with the experimental work of E. P. Herrero et. al. [12], where it was found experimentally that the particle size decreases when it is decreased the liquid flow. To justify this effect it should be taking into account that lower values of liquid flow rate result in thinner films. It was observed that thinner liquid films break down into smaller drops.

b) Air flow rate variation:

The influence of the air flow rate variation in the growth rate is shown in Figure 4. These results were obtained for an atomization nozzle of 1.8 mm in previous works conducted by the authors [12]. The experimental conditions were the following: a constant value of liquid flow of 0.009 L/min ($We_l = We_s = 0.11$) and the air flow rate was modified ranged from 89.600 L/min to 138.000L/min ($We_i = We_o = We_{si} = We_{so} = 14808$ to $We_i = We_o = We_{si} = We_{so} = 35128$). The liquid viscosity was maintained constant at 64.5 mPa s ($Z = 0.2$). It can be seen in Figure 4 that when the air flow increase, the growth rate increase, which indicates shorter breakup length and smaller drops.

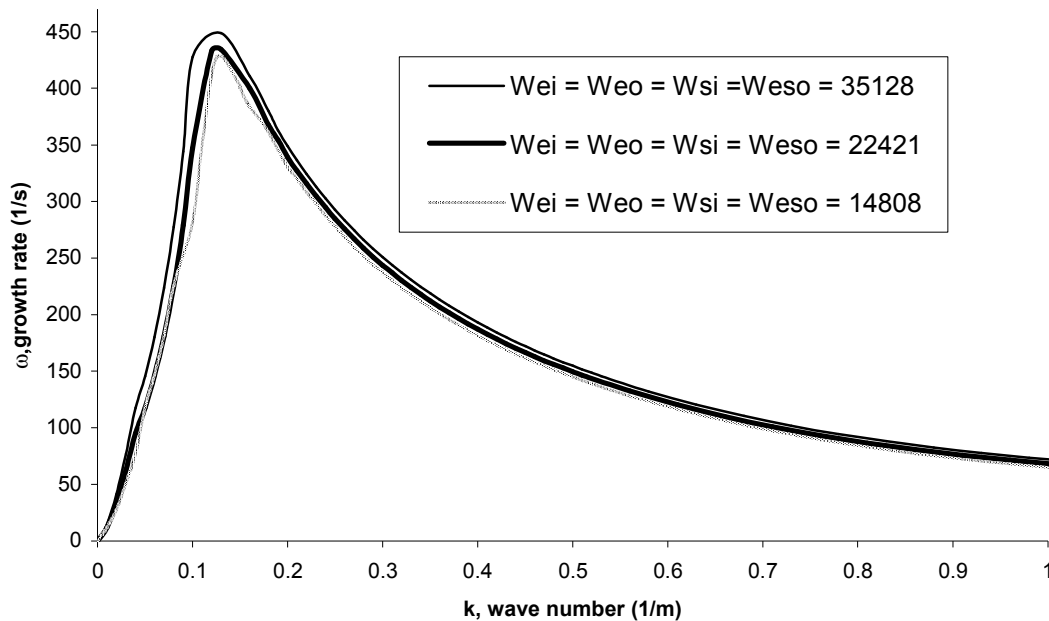


Figure 4: Dispersion diagram at

$We_l = We_s = 0.11; Z = 0.2$

$We_i = We_o = We_{si} = We_{so} = 14808 - 35128$

These results are in a very good agreement with the experimental work of E. P. Herrero et. al. [12], where it was found experimentally that the particle size decreases when it is increase the air flow. To justify this effect it should be take into account that the liquid/air interaction produces waves that become unstable and disintegrate into fragments. These fragments then, contract into ligaments, which in turn break

Instability study of an annular liquid sheet of polymer produced by atomization.

down into drops. It has been proved that when the air velocity is increased, the liquid sheet disintegrates earlier and ligaments are formed nearer the lip. These ligaments tend to be thinner and shorter and disintegrate into smaller drops. For a constant liquid sheet thickness the breakup length decreases with increase in the relative velocity between the air and the liquid.

c) Liquid viscosity effect:

The influence of the liquid viscosity in the growth rate is shown in Figure 5. These results were obtained for an atomization nozzle of 1.8 mm in previous works conducted by the authors [12]. The experimental conditions were the following: a constant value of pressurized flow air of 89.600 L/min ($We_i = We_o = We_{si} = We_{so} = 14808$), a constant value of liquid flow of 0.009 L/min ($We_l = We_s = 0.11$) and the liquid viscosity was modified ranged from 64.5 mPa s to 190.0 mPa s ($Z = 0.2$ to $Z = 0.6$).

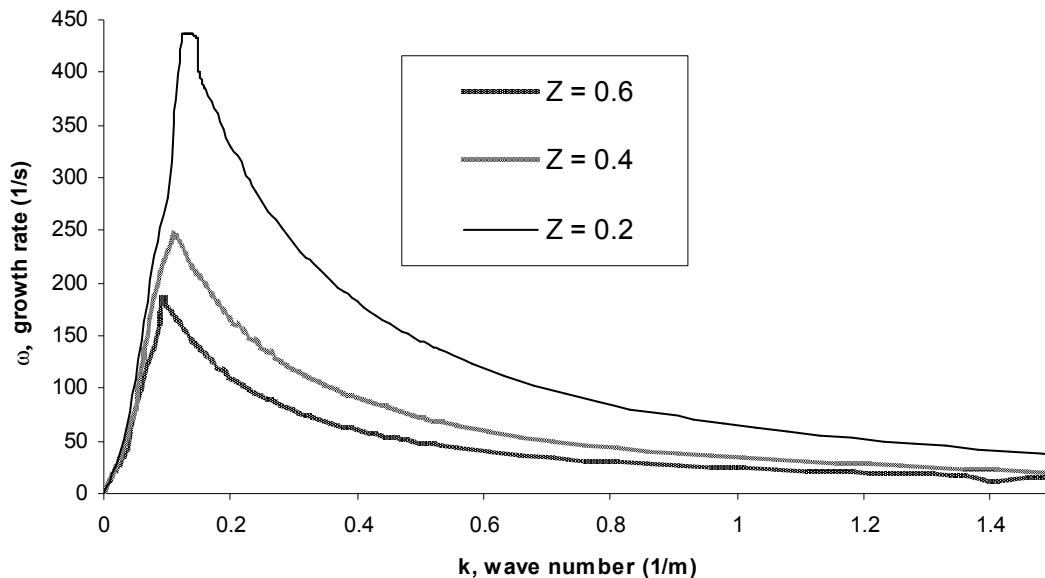


Figure 5: Dispersion diagram at

$We_i = We_o = We_{si} = We_{so} = 14808$; $We_l = We_s = 0.11$

$Z = 0.2 - 0.6$

It can be seen in Figure 5 that when the liquid viscosity decrease, the growth rate increase, which indicates shorter breakup length and smaller drops.

These results are in a very good agreement with the experimental work of E. P. Herrero et. al. [12], where it was found that the particle size increases when it was increased the liquid viscosity because of the viscosity of the liquid that is going to be atomized tends to prevent the growth of the instabilities that cause the rupture of the jet or liquid sheet, delaying, therefore, the disintegration of the liquid and increasing

the size of the microcapsules. In addition, lower values of liquid viscosity result in thinner films that break down into smaller drops.

5. Conclusions.

A temporal stability analysis is carried out to model the atomization of a swirling viscous annular liquid sheet emanating from an air-blast atomizer subject to inner and outer inviscid swirling air streams. The dimensionless dispersion equation that governs the instability of a viscous annular liquid sheet under swirling air streams is derived. Numerical solutions to the dispersion equation under a wide range of flow conditions are carried out to investigate the effects of the liquid and gas flow on the maximum growth rate. The growth rate can be related to the breakup length of the liquid sheet.

It has been observed that when the liquid flow decrease, the growth rate increase, which indicates shorter breakup length and smaller drops because of lower values of liquid flow rate result in thinner films that break down into smaller drops.

An analysis of the dispersion diagrams shows that when the air flow increase, the growth rate increase, which indicates shorter breakup length and smaller drops, because of the liquid/air interaction produces waves that become unstable and disintegrate into fragments, and contract into ligaments, which in turn break down into drops.

When the liquid viscosity decrease, the growth rate increases, this indicates shorter breakup length and smaller drops.

The theoretical behaviour predicted by the dispersion diagrams were compared with the experimental results obtained from the atomization of alginate solution using an air-blast atomizer. It was found that the instability model proposed justify the experimental effects found for the atomization of a fluid and under the work range for alginate flow rate and viscosity and air flow rate.

6. Nomenclature.

Symbol	Description	Units
A	Vortex Strength	m^2/s
D	Injector exit diameter, diameter of liquid jet	μm
$D_{0.9}$	diameter at the 90 th percentile	μm
$D_{0.1}$	diameter at the 10 th percentile	μm
$D_{0.5}$	diameter at the 50 th percentile	μm
D_a	Inner diameter of liquid sheet	μm
D_b	Outer diameter of liquid sheet	μm
g	Gas-to-liquid density ratio	
h	Ratio of inner and outer radius	
k	Axial wave number	$1/\text{m}$
n	Azimuthal wave number	
P	Mean pressure	N/m^2
p'	Disturbance pressure	N/m^2

Instability study of an annular liquid sheet of polymer produced by atomization.

Symbol	Description	Units
R_a	Inner radius of liquid sheet	m
R_b	Outer radius of liquid sheet	m
Z	Ohnesorge number, $\mu / (\rho_l \sigma D_b)^{1/2}$	
r	Radial coordinate	m
t	Time	s
U	Mean axial velocity	m/s
u	Disturbance axial velocity	m/s
V	Mean radial velocity	m/s
v	Disturbance radial velocity	m/s
W	Mean tangential velocity	m/s
We	Weber number ($We = \rho_l U^2 D_b / \sigma$)	
w	Disturbance tangential velocity	m/s

Greek letters

η	Displacement disturbance	m
μ	Fluid viscosity	Ns/m ²
ρ	Fluid density	kg/m ³
σ	Surface tension	kg/s ²
ω	temporal frequency	1/s
Ω	Angular velocity	1/s
θ	Azimuthal angle	radian
ϕ	Phase difference	radian

Subscripts

i	Inner gas
l	Liquid phase
o	Outer air
s	Based on swirling component

7. References.

- (1) Lefebvre, A. H., *Atomization and sprays*, Hemisphere, New York (1989).
- (2) Robitaille, R., et. al., (1999) *J. Biomed. Mater. Res.* 44, 116-120.
- (3) Orive, G., et. al., (2003) *Int. J. Pharm.* 259, 57-68.
- (4) Sugiura, S., et. al., (2005) *Biomaterials.* 26, 3327-3331.
- (5) Giffen, E., Muraszew, A., *The atomization of liquid fuel*, John Wiley, New York (1953).
- (6) Chigier, N., *Energy combustion and the environment*, McGraw-Hill, New York (1981).
- (7) Panton, R. L., *Incompressible flow*, John Wiley and Sons, New York (1995).

- (8) Adelberg, M., (1967) *AIAA J.* 5, 1408-1415.
- (9) Adelberg, M., (1967) *AIAA J.* 6, 1143-1147.
- (10) Jeffreys, H., (1925) *Proc. R. Soc. London A.* 107, 189.
- (11) Mayer, E., (1961) *ARS J.* 31, 1783-1785.
- (12) Herrero, E. P., Del Valle, E. M. M., Galán, M. A., (2006) *Chem. Eng. J.* 117, 137-142.
- (13) Herrero, E. P., Del Valle, E. M. M., Galán, M. A., (2006) *Chem. Eng. J.* 121, 1-8.
- (14) Jia, Y., Kanno, Y., Xie, Z-p., (2002) *J. Eur. Ceram. Soc.* 22, 1911-1916.
- (15) Rizk, N. K., Mongia, H. C. (1991) *J. Propul. Power.* 7, 305-311.
- (16) Shen, J., Li, X. (1996) *Acta Mech.* 114, 167-183.
- (17) Li, X., Tankin, R. S. (1991) *J. Fluid Mech.* 226, 425-443.
- (18) Liao, Y., Jeng, S. M., Jog, M. A. (2001) *J. Propul. Power.* 17, 411-417.
- (19) Chen, F. Tsaur, Y., Durst, F., Samir, K. (2003) *J. Fluid Mech.* 488, 355-367.